ELSEVIER

PII: S0032-3861(97)10324-X

Polymer Vol. 39 No. 15, pp. 3321–3326, 1998
© 1998 Elsevier Science Ltd
Printed in Great Britain. All rights reserved
0032-3861/98/$19.00+0.00

Crystal thicknesses in semicrystalline oxyethylene/oxybutylene block copolymers by atomic force microscopy and SAXS

I. W. Hamley[a,*], M. L. Wallwork[a], D. A. Smith[a], J. P. A. Fairclough[b], A. J. Ryan[b], S.-M. Mai[c], Y.-W. Yang[c] and C. Booth[c]

[a]*Centre for Self-Organising Molecular Systems, University of Leeds, Leeds, LS2 9JT, UK*

[b]*Department of Chemistry, University of Sheffield, Sheffield S3 7HF, UK*

[c]*Manchester Polymer Centre, Department of Chemistry, University of Manchester, Manchester M13 9PL, UK*

(Received 3 March 1997; revised 31 October 1997)

The structure of thin crystallized films of a diblock or a triblock copolymer deposited on silicon has been investigated using atomic force microscopy (AFM). Non-contact mode AFM was used to investigate the topography of crystallites of poly(oxyethylene)/poly(oxybutylene) (E/B) block copolymers at room temperature, where E is crystallized and B is amorphous. The crystal thicknesses determined from AFM were compared to bulk layer spacings determined using small-angle X-ray scattering (SAXS). This technique showed that $E_{41}B_{22}E_{41}$ (the subscript denotes the number of repeat units) largely crystallized in a monolayer with unfolded E blocks at the substrate and folded (looped) B blocks at the polymer–air interface, and with the E blocks tilted at an angle of *ca.* 60° relative to the substrate plane. Multiple layers with a common step height were observed for the diblock $E_{27}B_6$ crystallites, which were largely comprised of unfolded chains, also with E block tilted at an angle of *ca* 60° with respect to the substrate plane. © 1998 Elsevier Science Ltd. All rights reserved.

(Keywords: block copolymers; crystallization; atomic force microscopy)

INTRODUCTION

Crystallization in the bulk of semicrystalline block copolymers has been the subject of several recent papers[1–6]. For example, for a range of crystalline–amorphous diblock copolymers of poly(ethylene) and either poly(ethylethylene) ($T_g = -20$°C) or poly(ethylene-propylene) ($T_g = -56$°C), we have found that crystallization occurs in a lamellar structure whether the melt structure is lamellar or hexagonal-packed cylinders[1]. The lamellar period, and crystalline and amorphous PE domain thicknesses were determined from an analysis of the correlation function determined from synchrotron small-angle X-ray scattering (SAXS) experiments[1], whilst simultaneous WAXS was used to determine the crystal structure. In subsequent work, we studied chain folding in oriented poly(ethylene)-containing diblock copolymers using simultaneous SAXS/WAXS[4,5], and crystallization kinetics and thermodynamics in the same series of copolymers using SAXS[6].

We have also studied the crystal structure and morphology of semicrystalline diblock copolymers of poly(oxyethylene) and poly(oxybutylene) (abbreviated E_mB_n, where the subscript denotes the number of repeats) using simultaneous SAXS/WAXS/DSC[7,8]. These studies can be considered against a background of work on closely related E_mP_n diblock copolymers (P = oxypropylene)[9] and $E_mP_nE_m$ triblock copolymers[10], as well as $P_nE_mP_n$ triblock copolymers[11,12]. In all these copolymers, the E blocks crystallize in helical conformation[13], whilst the atactic B and P blocks are amorphous, but have been modelled in a trans-planar conformation[7].

Yang *et al.*[7] investigated $E_{30}B_n$ copolymers and found extended chain crystals for B block lengths $n \leq 13$ and lamellae containing once-folded E blocks for longer B blocks (B_{30}). Copolymers with intermediate block lengths formed mixed lamellae containing extended and folded E blocks. It was observed that for the copolymers with short B blocks the lamellar Bragg spacings from SAXS experiments were longer than their calculated molecular lengths. This was rationalized on the basis of irregular packing of fully-extended chains (oriented normal to the lamellar planes) so as to maintain normal crystalline-E and liquid-B densities.

Atomic force microscopy has been demonstrated by a number of groups to be an invaluable technique for characterization of nanoscale structures at the surface of block copolymer films[14–19]. Both contact and tapping mode™ (Digital Instruments, California) AFM have been employed for the investigation of surface topography[14–17], whilst contact mode AFM has been employed to study local friction and stiffness in glassy block copolymers[18,19]. Uniform thin films of block copolymers can be prepared by spin-casting materials onto a substrate wetted by the copolymer solution, followed by drying and subsequent annealing. The ultimate morphology is a function of copolymer composition, temperature, film thickness and surface tension of the blocks.

It is a general feature of block copolymer films that film thickness crucially affects the surface topography[14–19]. For non-crystalline lamellar block copolymers, extensive work using AFM and X-ray reflectivity has shown that if the film

* To whom correspondence should be addressed

Table 1 Characteristics of the block copolymers

	M_n(NMR)	M_w/M_n(GPC)	wt% E	mol% E	ϕ_{E_c}
$E_{27}B_6$	1630	1.05	73	82	0.69
$E_{41}B_{22}E_{41}$	5190	1.12	69	79	0.65

Molar mass ratio from GPC based on calibration with poly(oxyethylene) standards. ϕ_{E_c} = volume fraction E in crystalline state, calculated assuming densities of 1.21 and 0.97 g cm^{-3} for crystalline E and liquid B blocks[10,11]

thickness is not commensurate with the bulk layer spacing, the top layer breaks up into islands and holes so that the block copolymer may adopt its usual lamellar thickness subject to the constraint of conservation of material[15].

Block copolymers that do not wet the substrate flow into microscopic droplets that macroscopically appear hemispherical. However, AFM studies suggest that droplets of amorphous diblock copolymers can form terraces[16,17] due to the tendency for layer formation to overwhelm the surface free energy penalty associated with a stepped copolymer–air interface.

Pioneering contact mode AFM studies by Krausch *et al.* show that chemical sensitivity at the surface of thin films of glassy block copolymers (and also phase separated blends of glassy polymers) can be achieved by measuring microscopic friction and stiffness[18,19]. This provides invaluable information to complement topography on the nature of the block at the surface.

EXPERIMENTAL

Sample synthesis and characterization

The methods of copolymer synthesis and characterization are given elsewhere[20,21]. Copolymers were prepared by sequential anionic polymerization, and were characterized using gel permeation chromatography and ^{13}C NMR spectroscopy. The former gives the ratio of weight–average molecular weight to number average molar mass, M_w/M_n, and the latter the M_n values. Details of the block copolymers are presented in *Table 1*. As can be seen, the copolymers had narrow molar mass distributions ($M_w/M_n < 1.2$). The wider distribution of the triblock copolymer is discussed below.

Polymers were spun cast at 4000 rpm from solutions in dichloromethane (0.5–5 wt%) onto silicon wafers. The initial film thickness could be decreased by decreasing the concentration of polymer solution. Polished *n*-type silicon wafers (2″ diameter) with (111) orientation were cleaned with toluene and then acetone but were otherwise used as received from Semiconductor Processing Co., Boston, U.S.A.

Samples for SAXS were prepared by rapidly cooling from 80°C, which is above the melting temperature of poly(oxyethylene). Crystallization was then allowed to proceed at the final set temperature following the quench.

Atomic force microscopy

Atomic force microscopy images were obtained using a Nanoscope III(a) AFM (Digital Instruments, Santa Barbara, California) with a 16.5 × 16.5 micron scanning stage. All images were obtained in tapping mode™ using commercially available silicon nitride TESP tips. All images were obtained using the same tip. The only image processing performed on these images was a first order plane fit in the x and y directions.

Synchrotron X-ray scattering

SAXS experiments were performed on beamline 8.2 of the Synchrotron Radiation Source (SRS) at the Daresbury Laboratory, Warrington, U.K. Details of the storage ring, radiation, camera geometry and data collection electronics have been given elsewhere[22]. White radiation from the source was monochromated using a cylindrically bent Ge(111) crystal to give an intense beam of $\lambda = (1.50 \pm 0.01)$ Å X-rays. The beam was highly collimated to a typical cross-section of 0.3 × 4 mm^2 in the focal plane. The instrument was equipped with a multiwire quadrant detector for SAXS located 3.5 m from the sample position. A vacuum chamber was placed between the sample and detectors to reduce air scattering and absorption.

The samples for SAXS were prepared by placing isotropic pieces of copolymer cut from sheets in a cell comprising a Du Pont DSC pan fitted with windows (≈7 mm diameter) made from 5 μm thick mica. Sealed pans were placed in a spring loaded holder in a Linkam TMH600 hot-stage mounted on an optical bench. The design and operation of the X-ray DSC have been described in detail elsewhere[23]. The silver heating block of the hot-stage contained a 4 × 1 mm tapered slot which allowed the transmitted and scattered X-rays to pass through unhindered. The nominal cooling rate for quenches was 40°C min^{-1}.

A scattering pattern from an oriented specimen of wet collagen (rat-tail tendon) was used to calibrate the SAXS detector. A parallel plate ionisation detector placed before the sample cell recorded the incident intensities. The experimental data were corrected for background scattering (from the camera, hot stage and empty cell), sample absorption, and the positional alinearity of the detectors.

RESULTS AND DISCUSSION

Copolymer $E_{27}B_6$

Figure 1 shows a typical AFM image for a crystallite of $E_{27}B_6$, which is characterized by terraces of uniform polymer thickness. This is confirmed by the height profile in the cross-section shown in *Figure 1b*. The steps are (160 ± 10) Å in height, which is an average value including other regions of the specimen.

Representative SAXS data collected following quenches from the melt are shown for copolymer $E_{27}B_6$ in *Figure 2*. We have used the relationship $d = 2\pi/q^*$, where q^* is the position of the principal peak, to calculate lamellar spacings*. The lamellar periods for samples rapidly cooled to a crystallization temperature of 20°C or 25°C, were in the range d = 106–122 Å, the higher values corresponding to higher crystallization temperatures, with a mean value of $d \approx 110$ Å. A deeper quench to a crystallization temperature of 10°C gave $d \approx 90$ Å. In what follows we concentrate attention on the value of

* Use of the Bragg equation is an approximate means of determining the lamellar period. A complete analysis, using the correlation function method, is not possible, because this method can only be used for systems with a single lamellar period, and will not work for systems where there are mixed lamellae, such as the copolymer $E_{41}B_{22}E_{41}$ studied in this paper.

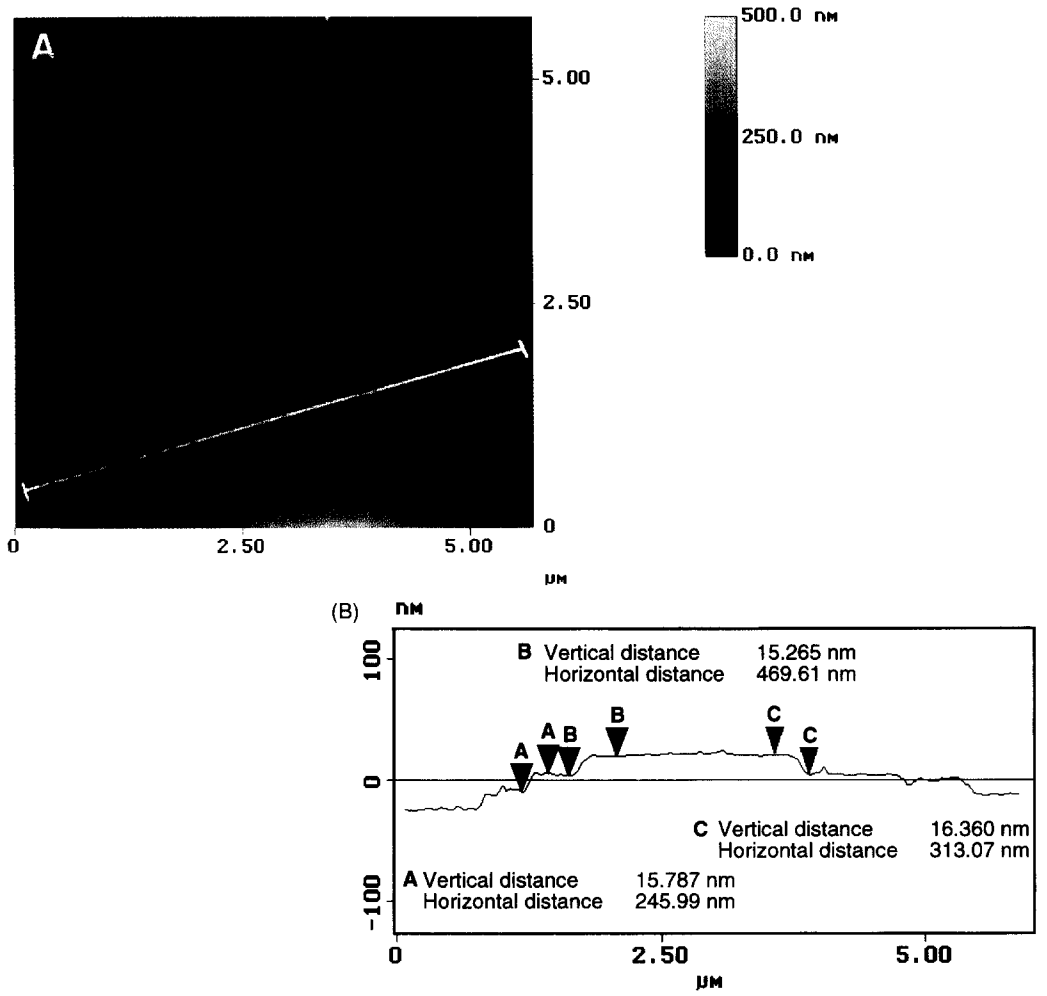

Figure 1 AFM of a crystal of $E_{27}B_6$ on silicon obtained at room temperature. (A) Two-dimensional image of a representative region of the sample, the line indicates where a height profile was measured. (B) Topography of steps, showing typical heights

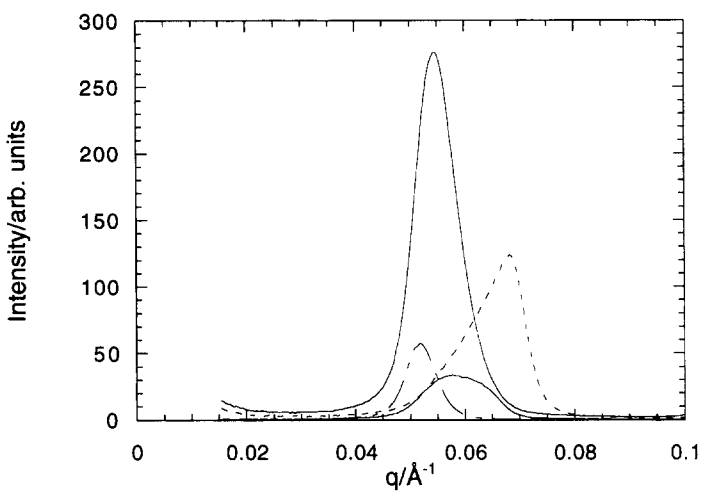

Figure 2 SAXS profiles for $E_{27}B_6$ following quenches from 80°C to 20°C (solid lines), 10°C (dashed line), 25°C (broken line). The latter two quenches and the quench to 20°C producing the small peak were at a nominal rate of 100°C/min. The first quench to 20°C was at 10°C/min

$d \approx 110$ Å found for the higher crystallization temperatures, assuming that this corresponds to more uniform lamellar stacks. Our previous report gives $d = 100$ Å for copolymer $E_{27}B_6$ crystallized under rather different conditions[7].

Two models were used to calculate d spacings for the E_mB_n copolymer. The general assumptions are that the E_m blocks are in helical conformation, are unfolded [as indicated by previous work[7], low-frequency Raman spectroscopy (LAM-1) and SAXS], and are oriented normal to the lamellar planes. An unfolded helical E_m block has length $2.85m$ Å, i.e. 77 Å for E_{27}[24].

Model 1: normal density. The assumption that the B block has its normal liquid density gives $d_1/\text{Å} = 77/\phi_{E_c}$, where ϕ_{E_c} is the volume fraction of the crystalline E blocks

in the lamella, ($\phi_{E_c} = 0.69$, see *Table 1*), i.e. $d_1 = 112$ Å, in excellent agreement with the value from SAXS.

Model 2: liquid crystal. The assumption that the B block is unfolded and in trans-planar conformation (essentially a liquid-crystal state) means that a B_n block has length $3.63n$ Å[7], i.e. 22 Å for B_6, yielding an overall length $d_2 = 99$ Å, which is somewhat lower than that found experimentally. Discrepancies of this kind were noted previously[7], and ascribed to irregular longitudinal packing of the unfolded chains, so as to reduce the overall density, i.e. to approach normal densities (Model 1). Nevertheless Model 2 (liquid-crystal model) has validity, since it has been shown to provide a consistent

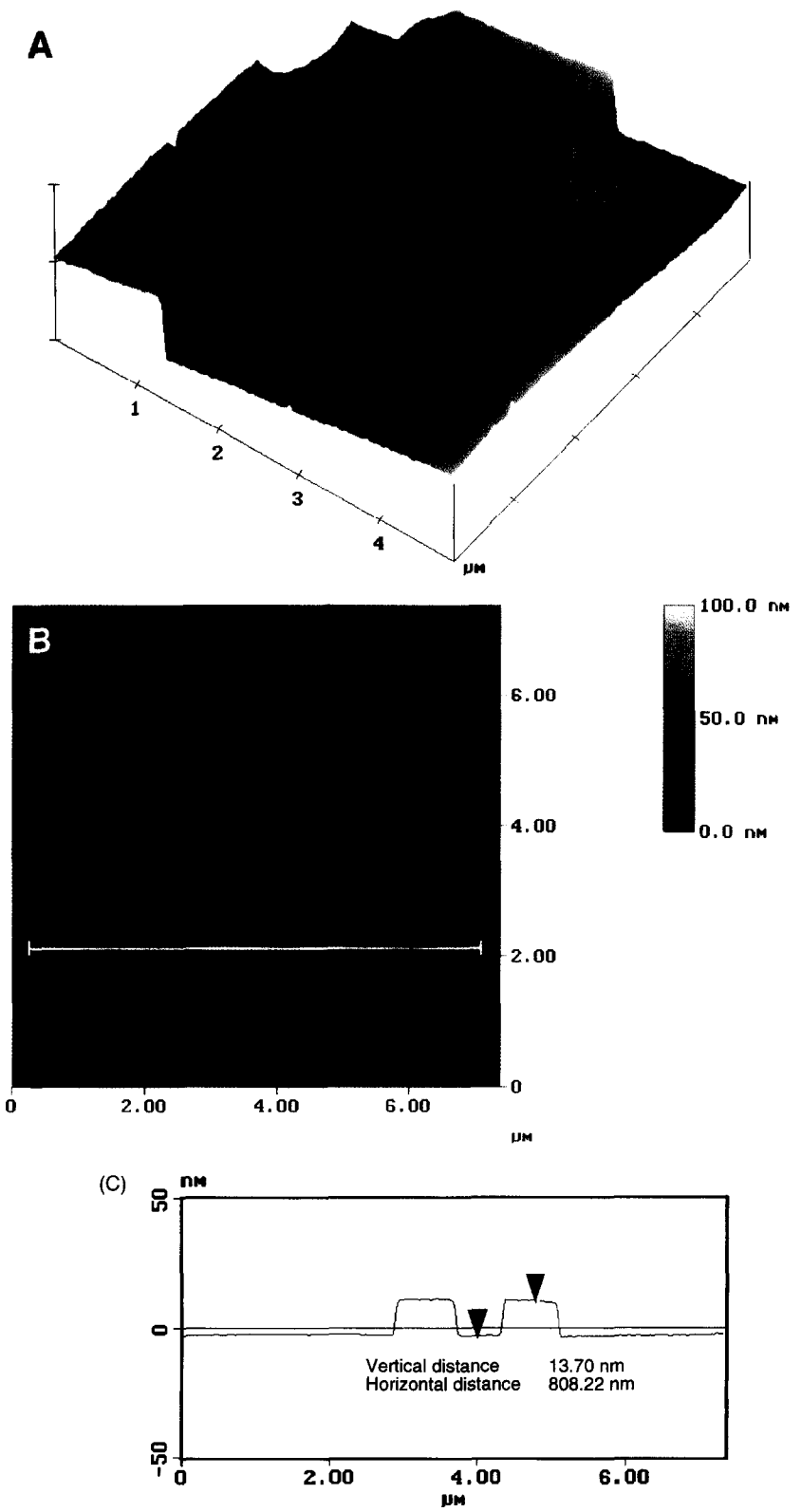

Figure 3 AFM of a crystal of $E_{41}B_{22}E_{41}$ on silicon. (A) Surface plot showing the edge of a monolayer crystal. (B) Two-dimensional image corresponding to the same area of the sample, the line indicates where a height profile was measured. (C) Topography of steps, showing typical height

explanation of the chain-length dependence of the LAM-1 frequencies found for the lower members of the $E_{30}B_n$ series[7].

The average step height for lamellae determined from AFM, 160 ± 10 Å, is significantly larger than the calculated d spacings. Two possible explanations are presented. One is that crystallization by evaporation of solvent in the thin film involves fractionation by E-block length, with a proportion of chains (*ca.* 30%) rejected into an amorphous surface layer. The second is that crystallization by evaporation of solvent allows formation of a bilayer, sandwiching an amorphous B-block layer between crystalline E-block layers, and that the E blocks in the bilayer are tilted away from the normal, i.e. a tilt angle of $\sin^{-1}(160/2d_2) = \sin^{-1}0.81 \approx 54°$ (see *Figure 5*) relative to the lamellar plane. Evidence of lamellar structures with tilted E blocks (SAXS and Raman spectroscopy) has been presented previously for bulk crystallized $P_nE_mP_n$ copolymers[12].

Copolymer $E_{41}B_{22}E_{41}$

Atomic force microscopy images from $E_{41}B_{22}E_{41}$ taken at room temperature are shown in *Figure 3*. The edge of a representative crystallite is shown in *Figure 3A*. This clearly shows that it has sharp edges, and is quite flat. A two dimensional plot of a larger area of a flat crystallite is shown in *Figure 3B*, showing smooth boundaries. A representative topographic profile for a section of this structure is shown in *Figure 3C*. This shows a step height of (140 ± 10) Å, which is typical of the step height measured for crystallites in other areas of the film.

Representative SAXS data collected following quenches from the melt are shown for copolymer $E_{41}B_{22}E_{41}$ in *Figure 4*. Quenching to 36°C resulted in a predominant peak in the SAXS pattern at 0.031 $Å^{-1}$, corresponding to a d spacing of approximately 200 Å. Quenching to 20°C gave a double peak, corresponding to $d \approx 170$ Å and 120 Å.

For copolymer $E_{41}B_{22}E_{41}$, the helical E-block length is 117 Å and the unfolded trans-planar B-block length is 80 Å, calculated as described above. The most likely conformation for this copolymer in a lamella is that of a once-folded chain, with the fold in the B block. In this conformation, the calculated d spacings are:

$$\textit{Model 1 (normal density)} : d_1 = 117/\phi_{E_c} = 180\,Å$$

$$\textit{Model 2 (liquid crystal)} : d_2 = 157\,Å$$

In contrast to the results for the diblock copolymer, for which d_1 (calculated) coincided in value with d (measured), the two quantities for the triblock copolymer show a significant discrepancy. A similar result was reported recently for copolymer $E_{33}P_{42}E_{33}$[10], and is attributed to the widened distribution of E-block lengths that results from polymerisation of ethylene oxide onto a precursor poly(oxypropylene) with secondary hydroxyl functional groups[25]. The same situation holds for $E_mB_nE_m$ copolymers, but the effect is more extreme[25,26]. The distribution width parameters (M_w/M_n) given in *Table 1* show the effect, with the values of 1.05 for $E_{27}B_6$ being consistent with a Poisson distribution of block lengths, while the value of 1.12 for $E_{41}B_{22}E_{41}$ signals a significantly wider distribution. Details

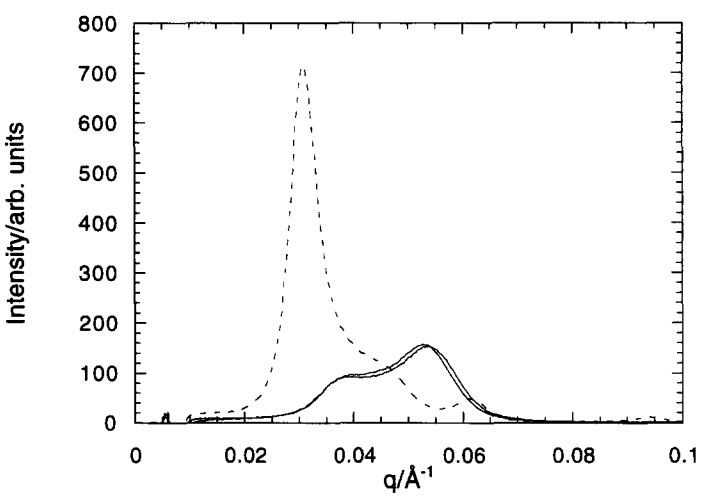

Figure 4 SAXS profiles for $E_{41}B_{22}E_{41}$ following quenches from 80°C to 20°C (solid lines) and 36°C (dashed line)

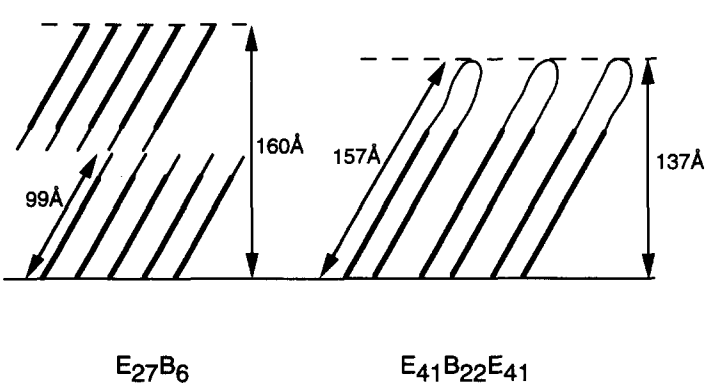

Figure 5 Schematic of tilt models for thin films of copolymers $E_{27}B_6$ and $E_{41}B_{22}E_{41}$ on silicon. The E block is shown as a thick line and the B block as a thin line

of the E-block-length distributions in copolymers $E_{41}B_8$ (Poisson) and B_8E_{41} (widened) have been presented elsewhere[25]. In the present case, a small proportion of the molecules of $E_{41}B_{22}E_{41}$ will have uncovered ends (i.e. no E block), and a significant proportion of E blocks will be short compared to expectation, with, in compensation, others being longer than expected. This means that a proportion of E blocks will not crystallize, so increasing the proportion of copolymer in the amorphous layer, hence its thickness, and also that the crystalline layer itself is composed of longer (on average) E blocks. An increase in d of 10–20% on this account is not unexpected, and is consistent with earlier work[10].

The smaller d spacings found for the more deeply quenched sample are consistent with a higher extent of folding. If both E blocks are folded as well as the B, the calculated spacings are $d_1 \approx 90$ Å and $d_2 \approx 100$ Å. Accordingly, we assign the $d \approx 120$ Å spacing to the fully folded (three-times folded) conformation and the $d \approx 170$ Å spacing to the once-folded structure, allowing, in each case, some latitude for the effect of E-block-length distribution and possible formation of mixed stacks.

The AFM measurements reveal a monolayer thickness, 137 ± 10 Å, that is significantly lower than the d spacing of the bulk crystallized material. Assuming this to be an effect of tilting, for the once-folded conformation the tilt angle is $\sin^{-1}(137/d_2) = \sin^{-1}(0.87) \approx 60°$, i.e. a value consistent (within experimental error, say ± 5°) with that derived for bilayers of diblock copolymer in the surface film.

The tilt angles used to explain the observed thickness of thin films of both polymers are consistent with tilting resulting from the displacement of an E chain by one unit in its monoclinic unit cell. Since the interchain distance in the monoclinic subcell is $b_0 = 4.62$ Å, a displacement of one E unit (2.85 Å) gives a natural tilt of $\tan^{-1}(4.62/2.85) = \tan^{-1}(1.62) = 58°$. This is the value expected for uniform chains. For non-uniform chains (essentially end melted) there will be some averaging, consistent with tilt angles in the range 54–60°. Thus the observation of layer spacings in thin films that differ from the bulk values can be explained on the basis of chain tilting, by displacement of E chains by one repeat unit. This is illustrated in *Figure 5* for both $E_{27}B_6$ and $E_{41}B_{22}E_{41}$. At present, it is uncertain whether the induced tilt is a result of specific interactions between the E block and the substrate, or whether it is an effect of crystallization in a thin film. Work is in progress on other E_mB_n polymers to investigate this further. Furthermore, we are performing grazing incidence diffraction experiments on thin films of EB diblocks to determine directly the extent of chain tilting, which should provide a direct test of the models discussed in this paper[27].

ACKNOWLEDGEMENTS

IWH, AJR and CB are grateful to the Engineering and Physical Sciences Research Council (U.K.) for the award of a grant which supported JPAF, and for the general support which underpinned the synthetic work. DAS acknowledges the support of the Leverhulme Trust and MLW the support of EPSRC. YYW is grateful for the support of the Government of the Republic of China, and SMM acknowledge the receipt of an ORS award.

REFERENCES

1. Ryan, A. J., Hamley, I. W., Bras, W. and Bates, F. S., *Macromolecules*, 1995, **28**, 3860.
2. Rangarajan, R., Register, R. A. and Fetters, L. J., *Macromolecules*, 1993, **26**, 4640.
3. Rangarajan, R., Register, R. A., Adamson, D. H., Fetters, L. J., Bras, W., Naylor, S. and Ryan, A. J., *Macromolecules*, 1995, **28**, 1422.
4. Hamley, I. W., Fairclough, J. P. A., Ryan, A. J., Bates, F. S. and Towns-Andrews, E., *Polymer*, 1996, **37**, 4425.
5. Hamley, I. W., Fairclough, J. P. A., Terrill, N. J., Ryan, A. J., Lipic, P., Bates, F. S. and Towns-Andrews, E., *Macromolecules*, 1996, **29**, 8835.
6. Hamley, I. W., Fairclough, J. P. A., Ryan, A. J., Bates, F. S., *Polymer*, 1998, **39**, 1429.
7. Yang, Y.-W., Tanodekaew, S., Mai, S.-M., Booth, C., Ryan, A. J., Bras, W. and Viras, K., *Macromolecules*, 1995, **28**, 6029.
8. Ryan, A. J., Fairclough, J. P. A., Hamley, I. W., Mai, S.-M. and Booth, C., *Macromolecules*, 1997, **30**, 1723.
9. Ashman, P. C. and Booth, C., *Polymer*, 1975, **16**, 889.
10. Fairclough, J. P. A., Yu, G.-E., Mortensen, K., Brown, W., Hamley, I. W., Sun, T., Booth, C. and Ryan, A. J., submitted to *Polymer*.
11. Ashman, P. C., Booth, C., Cooper, D. R. and Price, C., *Polymer*, 1975, **16**, 897.
12. Viras, F., Luo, Y.-Z., Viras, K., Mobbs, R. H., King, T. A. and Booth, C., *Makromol. Chem.*, 1988, **189**, 459.
13. Takahashi, Y. and Tadokoro, H., *Macromolecules*, 1973, **6**, 881.
14. van Dijk, M. A. and van den Berg, R., *Macromolecules*, 1995, **28**, 6773.
15. Maaloum, M., Ausserre, D., Chatenay, D., Coulon, G. and Gallot, Y., *Phys. Rev. Lett.*, 1992, **68**, 1575.
16. Ausserre, D., Raghunathan, V. A. and Maaloum, M., *J. Phys. France II*, 1993, **3**, 1485.
17. Carvalho, B. L. and Thomas, E. L., *Phys. Rev. Lett.*, 1994, **73**, 3321.
18. Meiners, J. C., Ritzi, A., Rafailovich, M. H., Sokolov, J., Mlynek, J. and Krausch, G., *Appl. Phys. A*, 1995, **61**, 519.
19. Krausch, G., Hipp, M., Böltau, M., Marti, O. and Mlynek, J., *Macromolecules*, 1995, **28**, 260.
20. Tanodekaew, S., Deng, N.-J., Smith, S., Yang, Y.-W., Attwood, D. and Booth, C., *J. Phys. Chem.*, 1993, **97**, 11847.
21. Yang, Z., Pickard, S., Deng, N.-J., Barlow, R. J., Attwood, D. and Booth, C., *Macromolecules*, 1994, **27**, 2371.
22. Bras, W., Derbyshire, G. E., Ryan, A. J., Mant, G. R., Felton, R. A., Lewis, R. A., Hall, C. J. and Greaves, G. N., *Nucl. Inst. Meth. Phys. Res. A*, 1993, **326**, 587.
23. Bras, W., Derbyshire, G. E., Cedie, J., Komanschek, B. E., Devine, A., Clark, S. M. and Ryan, A. J., *J. Appl. Cryst.*, 1995, **28**, 26.
24. Craven, J. R., Zhang, H. and Booth, C., *J. Chem. Soc., Faraday Trans.*, 1991, **87**, 1183.
25. Nace, V. M., Whitmarsh, R. H. and Edens, M. W., *J. Amer. Oil Chem. Soc.*, 1994, **71**, 777.
26. Yu, G.-E., Yang, Z., Ameri, M., Collett, J. H., Attwood, D., Price, C. and Booth, C., *J. Phys. Chem. B*, 1997, **101**, 4394.
27. Ryan, A. J., Fairclough, J. P. A., Terrill, N. J., Hamley, I. W. and Booth, C., in preparation.